



Application of photoactive electrospun nanofiber materials with immobilized *meso*-tetraphenylporphyrin for parabens photodegradation



M. Gmurek^{a,*}, M. Bizukojć^a, J. Mosinger^{b,c}, S. Ledakowicz^a

^a Faculty of Process and Environmental Engineering, Lodz University of Technology, Wolczanska 213, 90-924 Lodz, Poland

^b Faculty of Science, Charles University, Hlavova 2030, 128 43 Praha 2, Czech Republic

^c Institute of Inorganic Chemistry, v.v.i., Academy of Sciences of the Czech Republic, 250 68 Řež, Czech Republic

ARTICLE INFO

Article history:

Received 18 January 2014

Received in revised form 8 April 2014

Accepted 17 June 2014

Available online 11 July 2014

Keywords:

Esters of *p*-hydroxybenzoic acid
Heterogeneous photosensitized oxidation
Molecular singlet oxygen
Langmuir–Hinshelwood model
Photoactive materials

ABSTRACT

The pollution of aqueous environment by trace amounts of anthropogenic chemical substances has a hazardous impact on regular development of plants and animals as well as on human health. The paper presents the results of studies on the heterogeneous degradation of butyl- and benzylparaben in aqueous solutions using photochemically catalyzed processes. *Meso*-tetraphenylporphyrin (TPP) was immobilized in the polyurethane nanofiber material by electro-spinning method. The xenon lamp was used as a simulated sunlight source. The influence of various process parameters on reaction rate was investigated. The reuse of the carrier with the immobilized photosensitizer was examined. The major role of the singlet oxygen ($^1\Delta_g$) during the photodegradation was proved by using sodium azide and radical scavengers. The adsorption isotherms of parabens onto nanofiber material were determined using BET model. The kinetic study showed that the heterogeneous photodegradation of parabens could be modeled using Langmuir–Hinshelwood model and rate constants have been reported. The reaction pathway for the photodegradation of parabens via $^1\Delta_g$ was proposed.

© 2014 Elsevier B.V. All rights reserved.

1. Introduction

It has been known for over fifty years that the combination of molecular oxygen, visible light and some dyes leads to the oxidation of organic substances. The use of dye-sensitized photooxidation reaction in the field of medicine (photodynamic therapy [1,2]), chemistry (fine chemical synthesis [3,4]), environmental engineering (wastewater treatment [5,6]), etc. as a tool for the applications have stimulated research in this area. Two general photosensitized oxidation mechanisms are well known as: Type I also called radical-involving mechanism and Type II-singlet oxygen ($^1\Delta_g$) mechanism. It has been known that $^1\Delta_g$ can be used for water purification [7]. The immobilization of photosensitizers onto various materials is a desirable approach due to their easy separation from the reaction mixture and reuse. The immobilization of dyes could be associated with a decrease of $^1\Delta_g$ quantum yield. This may be due to the limitations in oxygen diffusion into and from the carrier material [8].

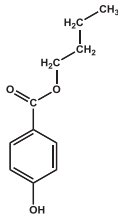
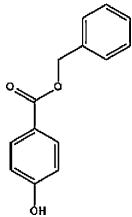
Immobilization of chromophores also leads to the maintenance of their molecular dispersion [9]. However, the process of chemical or physical bonding of photosensitizer with the carrier causes partial loss of activity. The first commercially available immobilized photosensitizer, Rose Bengal immobilized on Merrifield polymer, showed a 100-fold decrease in the efficiency of singlet oxygen generation [10]. Whereas, the works on tetra-phenylporphyrin (TPP) embedded in polyurethane (PUR) nanofiber showed that the photoactivity of the photosensitizer was probably dependent on the photosensitizer–carrier configuration. In a homogeneous aqueous solution of dissolved TPP the lifetime of $^1\Delta_g$ generated by the photosensitizer (3.5 μ s) is almost twice shorter than that in the heterogeneous system (6.3 μ s), aqueous solution in which TPP is incorporated into nanofibers [11]. Thus, the generation of $^1\Delta_g$ is possible by the use immobilized photosensitizer without the essential loss of its properties. Therefore, the immobilization of TPP onto polyurethane nanofibers is an original and innovative way to remove impurities from water environment.

Esters of *p*-hydroxybenzoic acid, commonly known as parabens are preservatives used in a variety of personal care products, cosmetics, pharmaceutical and food products. The presence of parabens was detected in wastewater, rivers, soil and house dust

* Corresponding author. Tel.: +48 42 631 37 93.

E-mail addresses: marta.gmurek@p.lodz.pl, marta.gmurek@gazeta.pl (M. Gmurek).

Table 1
Structure of n-butylparaben and benzylparaben and their toxicity [13].

Substances	Toxicity ($\mu\text{g dm}^{-3}$)		
	<i>D. magna</i> 48 h	<i>P. subcapitata</i> 72 h	<i>O. latipes</i> 96 h
<p><i>p</i>-Hydroxybenzoic acid <i>n</i>-butyl ester</p> 	<p>Acute toxicity EC₅₀</p> <p>1900</p> <p>Chronic toxicity–NOEC</p> <p>21 d</p> <p>800</p>	<p>9500</p> <p>72 h</p> <p>800</p>	<p>3100</p> <p>14 d VTG</p> <p>30</p>
<p><i>p</i>-Hydroxybenzoic acid benzyl ester</p> 	<p>Acute toxicity</p> <p>2100</p> <p>Chronic toxicity NOEC</p> <p>21 d</p> <p>840</p>	<p>1200</p> <p>72 h</p> <p>520</p>	<p>730</p> <p>14 d VTG</p> <p>20</p>

[12,13]. The potential hazard of parabens has been studied. The results obtained with *Daphnia magna* indicate on the toxicity of parabens towards the aquatic environment [14,15]. The toxicity and estrogenicity tests have shown that *p*-hydroxybenzoic acid benzyl ester (benzylparaben) is the most toxic and estrogenic compounds out of five studied parabens [16]. Butyl and benzyl esters of *p*-hydroxybenzoic acid exhibit both acute and chronic toxicity to algae (*Pseudokirchneriella subcapitata*), and fish (*Oryzias latipes*) (Table 1) [13] as well as to bacteria–*Vibrio fischeri* ($\text{LC}_{50} = 2.5 \text{ mg dm}^{-3} \rightarrow$ butylparaben ($\text{LOEC} = 0.7 \text{ mg dm}^{-3}$); $\text{LC}_{50} = 0.11 \text{ mg dm}^{-3} \rightarrow$ benzylparaben ($\text{LOEC} = 0.02 \text{ mg dm}^{-3}$), 15 min) [17].

Parabens can be considered as “pseudo-persistent” pollutants as a result of their continuous discharges into the environment throughout wastewater treatment and the issue of concern related to their eco-toxicological potencies [14–16].

Herein we present the results of photooxidation of butyl- and benzylparaben (Table 1) by visible light via $^1\Delta_g$ generated by immobilized TPP onto electrospun nanofibers material. The objective was to define the conditions that maximize the reaction rate of photosensitized degradation of parabens in the aquatic solution and to determine the kinetic model that describes the process in a heterogeneous system. Identification and analysis of toxicity of the products formed during the process were carried out as well.

2. Methods

p-Hydroxybenzoic acid *n*-butyl ester (>99%) (Butylparaben, BuP) and *p*-hydroxybenzoic acid benzyl ester (>99%) (Benzylparaben, BeP) were obtained from Fluka and Sigma-Aldrich, respectively. *Meso*-tetraphenylporphyrin (TPP) and zinc phthalocyanine (Zn-Pc) were photosensitizer were prepared by the electrospinning technique [18] and characterized in [11,19]. The study was carried out in a semi-continuous system in flat reactors ($6 \times 10 \text{ cm}$, 0.01 dm^3). The inner wall of the reactors was covered by nanofiber material in form of thin fabrics with the immobilized

photosensitizer. Reactors were symmetrically positioned around light source—a 100 W xenon lamp, simulating solar radiation. During the experiments the reaction mixture was agitated by a gentle air or oxygen stream. The BuP and BeP reaction decay was monitored by HPLC (Waters) with a UV diode array detector. A detailed detection procedure and experiment setup were previously published in [20]. The investigations were conducted at ambient temperature and the sample temperature was kept constant within $\pm 1^\circ\text{C}$ before and after the irradiation. The initial reaction rates were calculated by differentiating exponential curve that fitted experimental points for the first 30 min of reaction at the correlation factor higher than 0.97.

Identification of BuP and BeP photoproducts was done via ultra-high performance liquid chromatography with a diode array detector (UPLC[®] Acquity, Waters, USA) coupled in-line with a quadrupole–TOF hybrid mass spectrometer (Synapt G2, Waters, USA). Reversed phase chromatography was performed on an Acquity UPLC[®] BEH C18 column ($2 \text{ mm} \times 150 \text{ mm} \times 1.7 \mu\text{m}$) at 40°C (Waters) utilizing a gradient elution profile and mobile phase consisting of 0.1% formic acid in water (A) and 0.1% formic acid solution in acetonitrile (B) with the flow rate at 0.35 ml min^{-1} . The linear gradient elution profile composed of 5% solvent B for 2 min, from 5% to 15% B in 1 min, from 15% to 30% B in 2 min, from 30% to 50% B in 2 min, from 50% to 60% B in 3 min, and 60% B for 4 min. Analyzes were conducted in the negative (ESI-Q1) electrospray ionization. The capillary needle voltage was 3 kV as well as the source temperature was maintained at 120°C (ESI-Q1). Other volatages were as follows: sampling cone voltage, 40 V; extraction cone voltage, 4 V Desolvation gas (nitrogen) flow rate was 1000 l h^{-1} at 400°C . Cone gas flow was 100 l h^{-1} . Nitrogen was used as both the ESI nebulizer gas. Data acquisition was performed with a Waters MassLynx data system.

Toxicity of the BuP and BeP reaction solution before and after irradiation was analyzed using the commercially available ToxTrak test system (Hach, Loveland, CO, USA) and spectrophotometer Odyssey Hach[®]—model DR/2500 (Method 10017). For the

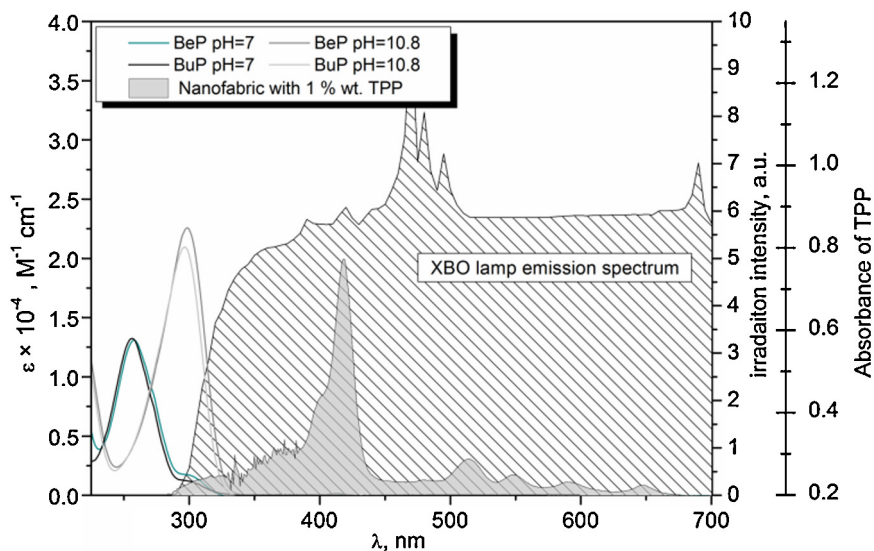


Fig. 1. Absorption spectra of parabens and TPP immobilized onto PUR nanofabric on the background of emission spectrum of xenon lamp.

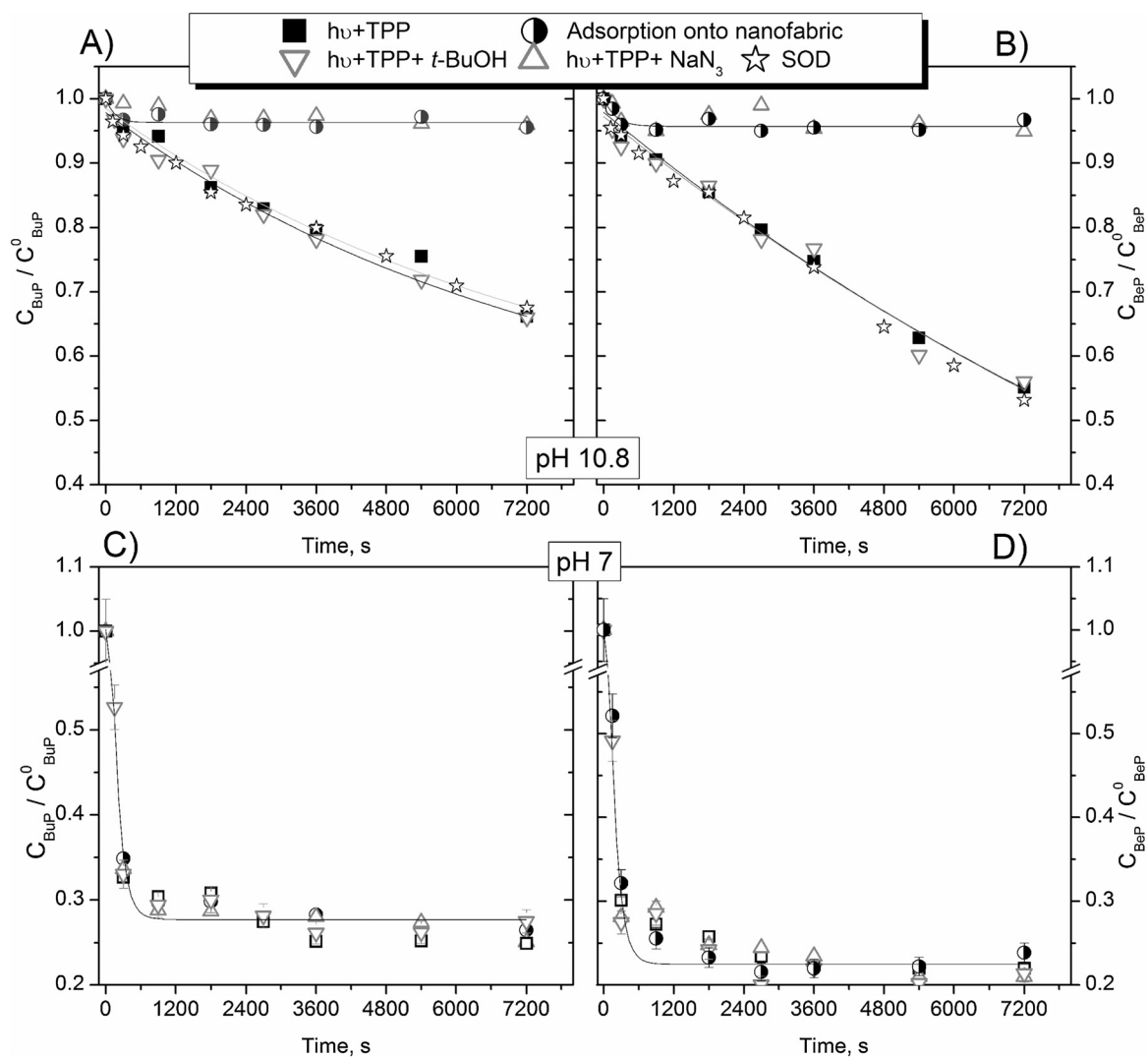


Fig. 2. Decay of BuP and BeP concentration at alkaline (A), (B) and neutral (C), (D) solution during photosensitized oxidation, adsorption parabens on nanofabrics and reaction in the presence of 0.02 M sodium azide, 0.1 M *t*-BuOH and 100 IU/ml SOD, $C_{\text{BuP/BeP}}^0 = 8 \times 10^{-5}$ M.

toxicological test Gram-negative bacteria (*Escherichia coli*, ATCC 8739) was used. The ToxTrak test is a colorimetric test based on the reduction of resazurin, a redox-reactive dye by bacterial respiration. Upon microbial respiration, blue resazurin is reduced to resorufin with a change of color into pink. The change in absorbance at 603 nm was measured spectrophotometrically and provided for a relative determination of percentage respiration inhibition.

3. Results

3.1. Preliminary study

Comparing the emission spectrum of the used Xe lamp and absorption spectra of parabens at neutral and alkaline solution (Fig. 1), the occurrence of partial photolysis can be suspected.

The performed experiments in neutral solution in the absence of the photosensitizer indicated on about 4% and 10% degradation of BuP and BeP due to photolysis, respectively. In alkaline solutions the irradiation caused to decreasing of BuP and BeP concentrations by 0.5% and 7%, respectively. The absorption spectrum of TPP immobilized onto PUR nanofiber material showed that it can efficiently absorb radiation emitted by xenon lamp. The calculated photon fluence of polychromatic light entering the reaction space was equal to $E_0^{7\text{cm}} = 554 \mu\text{E s}^{-1} \text{dm}^{-3}$ and $E_0^{11\text{cm}} = 324 \mu\text{E s}^{-1} \text{dm}^{-3}$. The TPP incorporated in PUR nanofibers at the concentration of 1% wt. TPP used in experiments absorbed $E_a^{7\text{cm}} = 87.5 \mu\text{E s}^{-1} \text{dm}^{-3}$ and $E_a^{11\text{cm}} = 51.1 \mu\text{E s}^{-1} \text{dm}^{-3}$.

3.2. Influence of process parameters

The series of experiments were conducted to examine the differences in the kinetic behavior of the heterogeneous photosensitized oxidation in alkaline and neutral solutions. In the first step of study the effect of absence or presence of radiation on the reaction were carried out. The study of photodegradation pathways was performed in the presence of reactive oxygen trappers. Sodium azide was used as a water-soluble physical quencher of $^1\Delta_g$ [21], *t*-BuOH as hydroxyl radicals scavenger [22] and superoxide dismutase (SOD) as a scavenger of superoxide radical ($\text{O}_2^{\bullet-}$) [23].

Addition of NaN_3 to the reaction solution led to total inhibition of parabens degradation (Fig. 2) in the alkaline solution however in the neutral environmental solution there was no impact on the extent of parabens concentration reductions. The experiments performed in the presence of *t*-BuOH as well as SOD did not cause any changes in the reaction run in both neutral and alkaline solutions. The observed influence of the additives on parabens decay rate demonstrated a dominant role of the singlet oxygen reaction with BuP and BeP in the alkaline solution but in the neutral solution the presence of $^1\Delta_g$ as well as hydroxyl radicals were not observed (no reaction with NaN_3 and *t*-BuOH). As it can be seen in Fig. 2, the photodegradation occurred only in the alkaline solution while in the neutral solution parabens adsorbed on the carrier.

The important parameter influencing the reaction rate of the photosensitized oxidation process is the concentration of photosensitizer immobilized into polyurethane nanofibers. In order to investigate this relationship, a series of experiments with nanofibers material incorporated with various TPP weight concentrations: 0.1%, 0.5% and 1% was carried out. The influence of the presence of 0.3 wt% zinc phthalocyanine (Zn-Pc) immobilized onto the same carrier was also examined. The use of different concentrations of the immobilized TPP into nanofiber material showed that with the increasing amount of photosensitizer the reaction rate increased (Fig. 3A). The higher concentration of TPP in nanofibers material caused the higher degradation of parabens. The important finding of these studies is that the use of even a small addition of

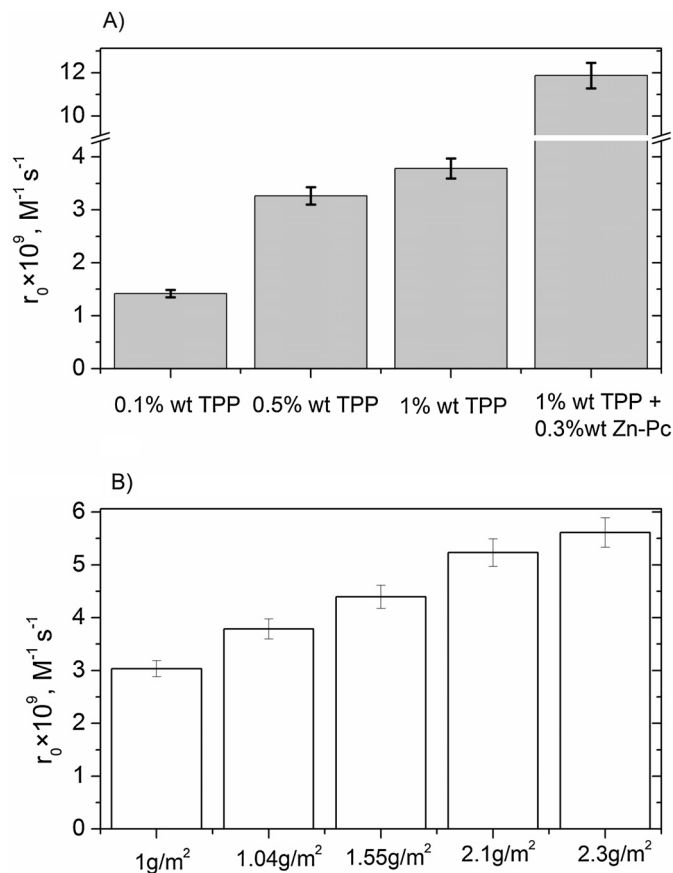


Fig. 3. Dependence of the initial BuP reaction rate (r_0) upon (a) different % wt. of photosensitizer concentration: (the area weight for 0.1%wt.–1%wt. TPP was 1.04 g/m², for mixture of photosensitizer nanofabrics—2 g/m²); (b) different area weight for nanofabric 1%wt.TPP.

Zn-Pc resulted in the significant acceleration of the reaction rate. It should be noted, that nanofibers material with a mix of photosensitizers had area weight significantly higher (2 g/m²) than the carrier with the same amount of TPP—1.04 g/m². It was therefore necessary to check the effect of the nanofibers material area weight on the photosensitized reaction rate (Fig. 3B).

As it can be seen in Fig. 3, the use of different area weights of nanofibers accelerates the reaction rate. The application of the nanofibers material with the highest area weight (2.3 g/m²) under the same reaction conditions led to the 24% increase of BuP degradation efficiency and 85% increase of BuP reaction rate, compared to the nanofibers material with lowest area weight (1.00 g/m²). The use of a larger area weight did not affect the mechanism of the process (which was confirmed by experiments with sodium azide).

The great advantage of the immobilized photosensitizers is the possibility of their reuse. A series of experiments was performed with the same nanofibers material several times. The possibility of the manifold application was examined by comparing the relative decrease in BuP concentration after each use of nanofibers material using different light intensity. The changes of BeP concentrations after irradiation of nanofibers material containing 1%wt. TPP and 0.3%wt. Zn-PC were followed. After each use the nanofibers material were rinsed with distilled water and dried under ambient conditions. The solutions of the same concentration have been oxygenated by air and exposed to radiation. As it is shown in Fig. 4, the nanofibers material can be used several times but each subsequent use results in lower efficiency of photodegradation. The increase of the photon flux entering the reaction space led to the higher parabens decay rate.

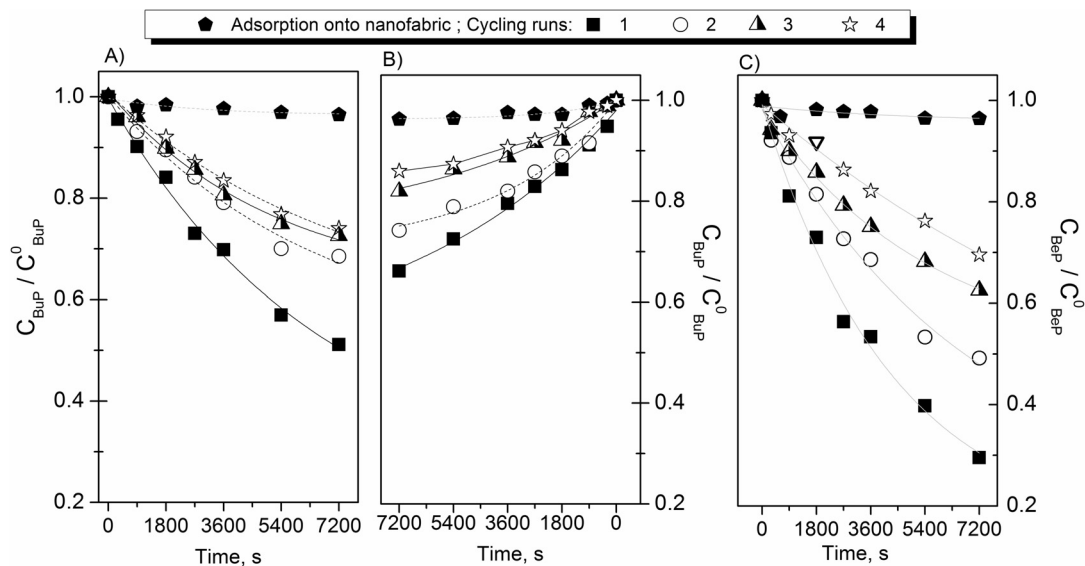


Fig. 4. Cycling runs of photosensitized oxidation (A) BuP ($E_0^{7\text{cm}} = 554 \mu\text{E s}^{-1} \text{dm}^{-3}$, 1%wt. TPP, 2.1 g/m²), (B) BuP ($E_0^{11\text{cm}} = 324 \mu\text{E s}^{-1} \text{dm}^{-3}$, 1%wt. TPP, 2.1 g/m²), (C) BeP ($E_0^{11\text{cm}} = 554 \mu\text{E s}^{-1} \text{dm}^{-3}$, 1%wt. TPP+0.3 wt. Zn-Pc, 2.0 g/m²).

After the first irradiation ($E_0^{7\text{cm}} = 554 \mu\text{E s}^{-1} \text{dm}^{-3}$) of nanofibers material with 1% wt. TPP approximately 50% loss of initial BuP concentrations was achieved, for lower photon flux ($E_0^{11\text{cm}} = 324 \mu\text{E s}^{-1} \text{dm}^{-3}$) 35% of BuP concentration decay was observed. After a four-fold use of nanofibers material the efficiency of photodegradation was about twice lower. The decrease of BuP concentrations was equal 26% and 14% for $E_0^{7\text{cm}}$ and $E_0^{11\text{cm}}$, respectively. The application of the mixture of photosensitizers into nanofibers material (1%wt. TPP+0.3 wt. Zn-Pc) gave higher degrees of reduction. At the first exposure about 70% decrease of BeP concentration was achieved. The second time about 51% degradation of BeP was reached, for the third—about 37%, and for the fourth approximately 30% of BeP concentration was removed.

The observed decreases in the operating efficiency of photosensitizers immobilized into nanofibers material was probably the result of their autobleaching initiated by light. After 8 h of nanofibers material irradiation apparent decrease in luminescence dyes was observed, which could be due to their bleaching and decreasing the activity in the generation of $^1\Delta_g$. The reuse of nanofibers material also resulted in changes in its structure, as well as decreased mechanical resistance to damage.

3.3. Kinetic studies

In order to determinate the kinetics of photosensitized oxidation process in the heterogeneous condition, the amount of adsorbed pollutant was examined. The adsorption isotherm of BuP and BeP onto nanofibers material at alkaline solution were determined using Brunauer-Emmet-Teller (BET) equation in the liberalized form:

$$\frac{1}{q_e(1-X)} = \frac{1}{q_{\text{max}}} + \left(\frac{1-X}{X}\right) \frac{1}{q_{\text{max}}K_{\text{BET}}} \quad (1)$$

where $X = C^e/C^s$, q_{max} is the amount of adsorbed paraben which takes place in a complete monolayer [mol g^{-1}], q_e is amount of appropriate paraben adsorbed onto nanofibers material at equilibrium (mol g^{-1}). C^s is the saturated solubility of appropriate paraben in water, C^e is appropriate paraben equilibrium liquid-phase concentration. K_{BET} is the equilibrium constant characterizes the interaction energy of adsorbate with the surface of adsorbent.

In the heterogeneous system the most frequently used kinetic model to formulate photodegradation rate equations is

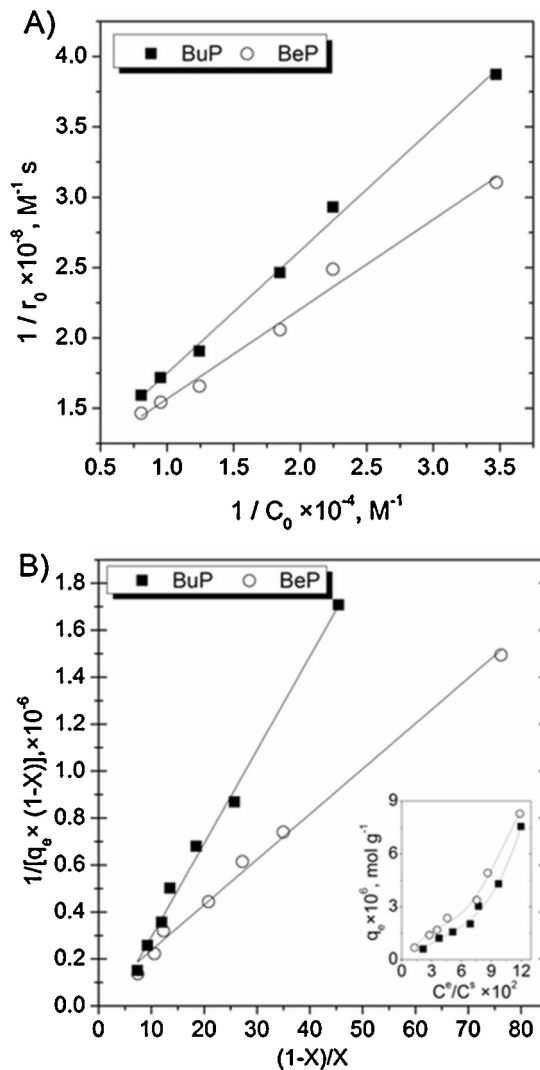


Fig. 5. (A) Linearization of Langmuir–Hinshelwood's equation for BuP and BeP, 1%wt. TPP, $E_0^{7\text{cm}} = 554 \mu\text{E s}^{-1} \text{dm}^{-3}$, $C_{\text{O}_2} = 0.27 \text{ mM}$, $\text{pH} = 10.8$; (B) Linearized BET isotherm for BuP and BeP adsorption onto nanofibers 1 wt% TPP 2.1 g/m². Inset: The isotherm of adsorption.

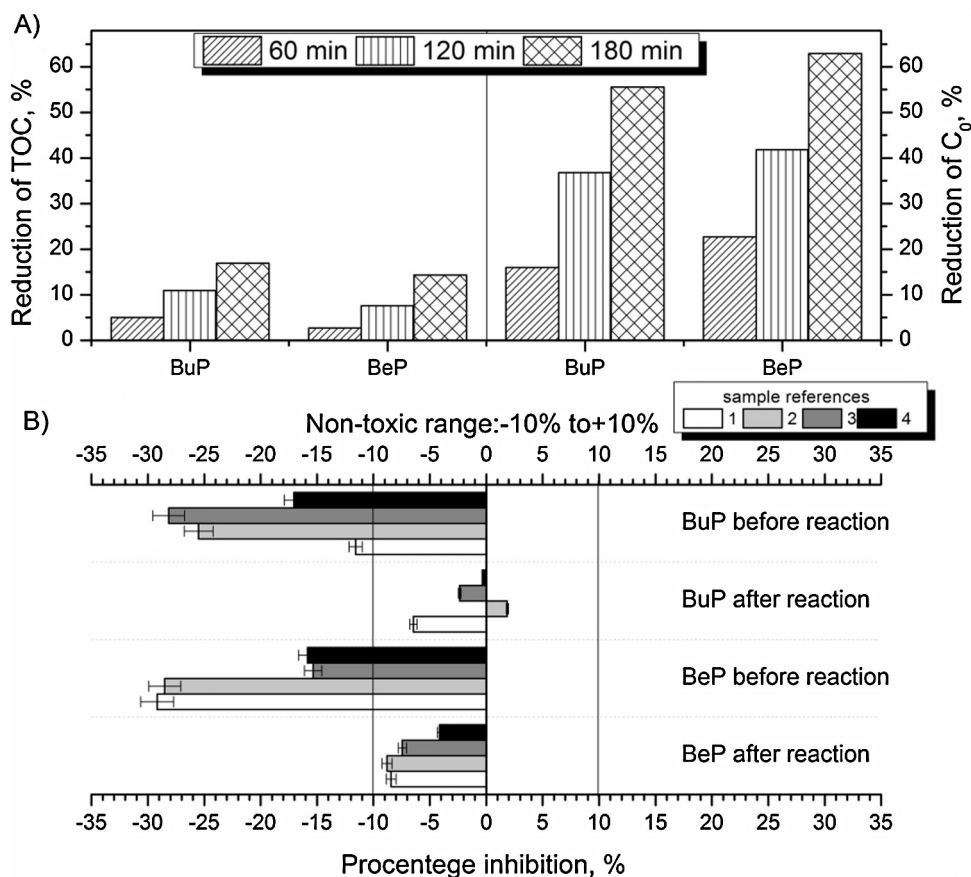


Fig. 6. (A) TOC and initial concentration decreases during the photosensitized oxidation. (B) Changes in toxicity (as measured by inhibition *E. coli*) before treatment and after 180 min of radiation in the presence of TPP incorporated into PUR nanofabrics, $C_{\text{BuP}}^{\circ} = 4 \times 10^{-4}$ M, $C_{\text{BeP}}^{\circ} = 4 \times 10^{-4}$ M, $\text{TOC}_{\text{BuP}}^{\circ} = 56.93$ ppm, $\text{TOC}_{\text{BeP}}^{\circ} = 69.15$ ppm, $E_0^{\text{cm}} = 554 \mu\text{E s}^{-1} \text{dm}^{-3}$, $C_{\text{O}_2} = 0.27$ mM, pH = 10.8.

Langmuir-Hinshelwood model [24–26]. This model assumes that the reactions take place at the surface of the carrier, and the reaction rate is proportional to the fraction of the surface covered by the reactant. L-H model describes the competitive adsorption of substrate, reaction intermediates and photodegradation products, moreover assumes that all intermediate photoproducts have the same binding characteristics to the immobilized photosensitizers as the main substrate [27,28]. The simplify L-H model can be used to explain the relation between the initial reaction rates and the contaminant concentration after adsorption equilibrium was achieved:

$$\frac{1}{r_0} = \frac{1}{k_{\text{LH}}} + \frac{1}{Kk_{\text{LH}}} \left(\frac{1}{C_0} \right) \quad (3)$$

where k_{LH} is the apparent reaction rate constant, K is the dynamic equilibrium constant of parabens adsorption onto nanofibers material.

The results were described successfully by Langmuir-Hinshelwood (L-H) model (Fig. 5A). A BET isotherm was also used to fit the adsorption data according to the linear form of isotherm model (Eq. 2) (Fig. 5B). The parameters of BET as well as kinetic L-H parameters are presented in Table 2. The high values of determination coefficients (above 0.99) indicated the good fitting

of experimental data, allowing the use of these models to predict process performance.

3.4. Toxicity results

Analysis of the content of total organic carbon (TOC) for both parabens and its decrease during the photosensitized oxidation process was performed. The samples were analyzed during the process after 60 min, 120 min and 180 min in the alkaline environment. As it can be seen from Fig. 6A, despite a significant decrease in the initial concentration of parabens their mineralization is minimal, implying the necessity to examine intermediates and their toxicity.

This part of experiments was focused on the comparison of the toxicities of pure paraben reaction solution before irradiation and reaction solution containing photoproducts, which were formed as a result of 180 min treatment. Toxicity tests were based on a colorimetric method (ToxTrak). *Escherichia coli* was used as the test bacterial strain. Each sample containing appropriate paraben before or after the process was prepared in four series and compared with a control sample. Such comparison allows for the determination of the background inhibition under the specific

Table 2
Values of parameters of BET isotherms and L-H kinetic parameters.

	BET isotherm			Langmuir-Hinshelwood model		
	q_{max} (mol g^{-1})	K_{BET} (-)	R^2 (-)	k_{LH} (M s^{-1})	K (M^{-1})	R^2 (-)
BuP	1.00×10^{-5}	2.55	0.994	$(1.217 \pm 0.024) \times 10^{-8}$	9109 ± 182	0.995
BeP	2.23×10^{-5}	2.32	0.993	$(1.077 \pm 0.043) \times 10^{-8}$	14552 ± 582	0.993

Table 3
Photoproducts of the photosensitized oxidation of parabens identified by UPLC–qTOF-MS.

No.	Molecular formula	Compounds	Retention time, min	Analyzed mass of M-H ion m/z	Real monoisotopic mass of M-H ion m/z	Absolute error of determination of mass of M-H ion	Main fragments
Butylparaben							
1	C ₁₁ H ₁₄ O ₃	Butylparaben ^a	9.88	193.0883	193.0943	-0.0060	→137.0251, 93.0325
2	C ₇ H ₆ O ₃	p-Hydroxybenzoic acid ^a	5.62	137.0251	137.0317	-0.0066	→93.0325
3	C ₇ H ₆ O ₅		5.30	168.9900	169.0215	-0.0315	
4	C ₇ H ₆ O ₇		2.36	200.9858	201.0113	-0.0255	
5	C ₆ H ₆ O	Phenol ^a	5.58	93.0367	93.0419	-0.0052	→76.0546, 66.0321
6	C ₆ H ₆ O ₂	Hydroquinone ^a	1.98	109.0438	109.0368	+0.0070	→81.0427
7	C ₆ H ₄ O ₂	1,4-Benzoquinone	1.78	108.0218	108.0211	-0.0007	→95.0121
8	C ₁₁ H ₁₄ O ₄	Dihydroxybenzoic butyl ester	8.21	209.0923	209.0892	+0.0034	→153.0295
9	C ₇ H ₆ O ₄	2,4-Dihydroxy benzoic acid; 3,4-Dihydroxy benzoic acid	3.06; 3.12	153.0295	153.0266	+0.0029	→109.0283, 78.9601
10	C ₆ H ₄ O ₃	2-Hydroxy (1,4) benzoquinone ^a	3.20	123.0076	123.016	-0.0084	→108.0218, 95.0121
Benzylparaben							
1	C ₁₄ H ₁₂ O ₃	Benzylparaben ^a	9.95	227.0687	227.0787	-0.0100	→137.0251, 93.0325
2	C ₇ H ₆ O ₃	p-Hydroxybenzoic acid ^a	5.62	137.0251	137.0317	-0.0066	→93.0325
3	C ₇ H ₆ O ₅		5.30	168.9900	169.0215	-0.0315	
4	C ₇ H ₆ O ₇		2.36	200.9858	201.0113	-0.0255	
5	C ₆ H ₆ O	Phenol ^a	5.58	93.0367	93.0419	-0.0052	→76.0546, 66.0321
6	C ₆ H ₆ O ₂	Hydroquinone	1.98	109.0438	109.0368	+0.0070	→81.0427
7	C ₆ H ₄ O ₂	1,4-Benzoquinone	1.78	108.0912	108.0211	-0.006	→95.0121
8	C ₁₄ H ₁₂ O ₄	Dihydroxybenzoic benzyl ester	8.83	243.0661	243.0736	-0.0075	→153.0295
9	C ₇ H ₆ O ₄	2,4-Dihydroxy benzoic acid ^a ; 3,4-dihydroxy benzoic acid ^a	3.06; 3.12	153.0295	153.0266	+0.0029	→109.0283, 78.9601
10	C ₆ H ₄ O ₃	2-Hydroxy (1,4) benzoquinone ^a	3.20	123.0076	123.016	-0.0084	→108.0218, 95.0121

^a Analyzed by the standard.

conditions, in which the sample was prepared, and the correct calculation of the inhibition of *E. coli* activity. The respiration inhibition was calculated with the following equation:

$$\% \text{ Inhibition} = \left[1 - \frac{\Delta A_{\text{sample}}}{\Delta A_{\text{control}}} \right] \times 100 \quad (4)$$

After 180 min of the photosensitized oxidation process of BuP and BeP, the toxicity of the reaction solution were significantly decreased for both cases (Fig. 6B). On the basis of the proposed methodology (ToxTrak) it can be stated that the solutions contained non-toxic reaction products. It is known from literature that benzylparaben is more toxic than butylparaben (Table 1), our results confirmed this knowledge and indicated that BeP photoproducts occurred to be more toxic.

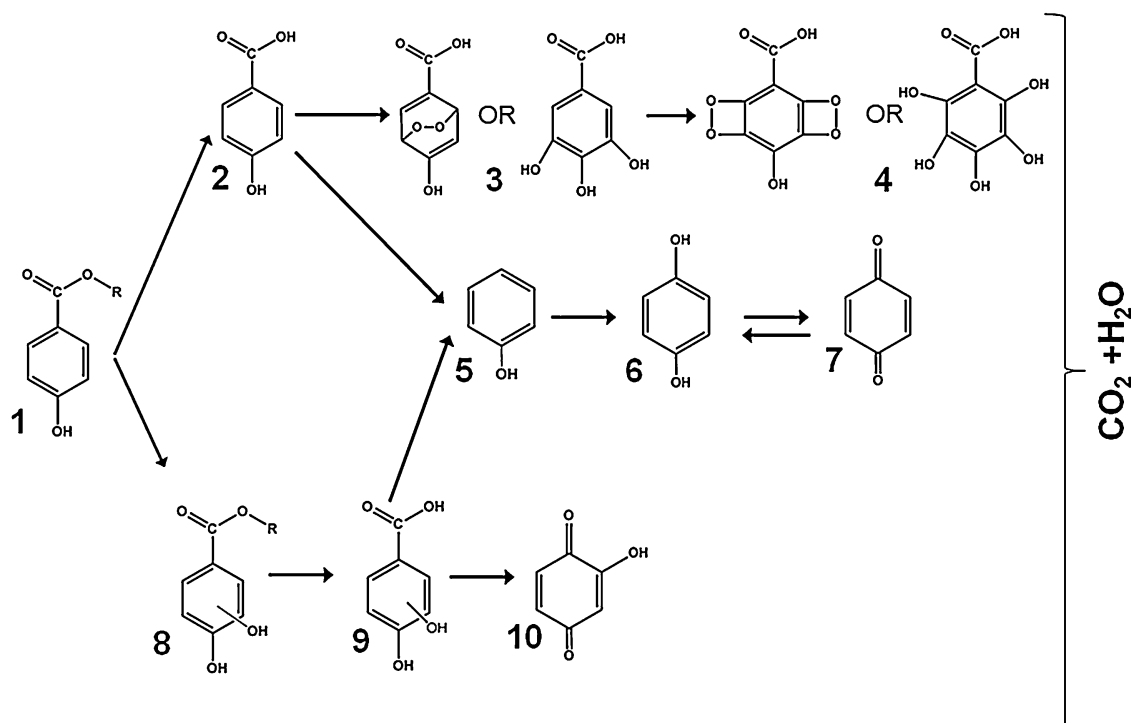


Fig. 7. Proposed reaction pathway for parabens photodegradation via singlet oxygen; BuP, R=CH₂CH₂CH₃; BeP, R=CH₂C₆H₅.

3.5. Identification of photoproducts

The UHPLC-qTOF-MS analysis allowed for the identification of the main products formed during parabens degradation. In order to determine the intermediates formed during the photosensitized oxidation of parabens the reaction solution was irradiated for 30, 60, 120, 180 and 240 min in the presence of nanofibers material containing 1% wt. TPP and 0.3% wt. Zn-Pc. It is known that parabens undergo hydrolysis to p-hydroxybenzoic acid (4-HBA). In order to test this hypothesis, also the photodegradation of 4-HBA by $^1\Delta_g$ was examined. In addition, phenol, hydroquinone, 2-hydroxy (1,4) benzoquinone, 2,4-dihydroxybenzoic acid, 3,4-dihydroxybenzoic acid as the intermediates were also identified by UHPLC-MS analysis. All studies were carried out at pH 10.8 using a light intensity equal to $554 \mu\text{E s}^{-1} \text{dm}^{-2}$. The main photoproduct of BuP and BeP photodegradation was 4-hydroxybenzoic acid formed by the hydrolysis of parabens. In the subsequent stages the 4-HBA was degraded to a compound of the formula $\text{C}_7\text{H}_6\text{O}_5$. Due to the mechanism of the $^1\Delta_g$ reaction with organic compounds it may be a compound formed by the attachment of singlet oxygen or hydroxyl groups. The second main degradation product was dihydroxybenzoic butyl ester (for BuP) and dihydroxybenzoic benzyl ester (for BeP), which resulted from hydroxylation of parabens. The analysis indicates that 2,4-dihydroxybenzoic acid as well as 3,4-dihydroxybenzoic acid are the photo-products of photosensitized oxidation of BuP and BeP.

The degradation of the intermediates *via* $^1\Delta_g$ led to the formation of hydroquinone and 1,4-benzoquinone, which could be easily broken down into simple non-aromatic compounds by the cleavage of aromatic ring.

Table 3 shows all the identified photoproducts formed during the reaction of parabens with the $^1\Delta_g$. The low values of the absolute error of determination of masses of all ions indicated that their identification is reliable. Owing to the analysis of the reaction intermediates the pathway of paraben degradation by singlet oxygen was proposed (Fig. 7).

4. Conclusion

Polyurethane polymer nanofibers material with the immobilized *meso*-tetraphenylporphyrin are capable of degrading parabens in the presence of visible light and molecular oxygen. The major role in this process plays singlet molecular oxygen. The degradation occurs due to Type II reaction mechanisms. The efficiency of the parabens removal is strongly dependent on pH level of the reaction solution, the initial photosensitizers concentration as well as the nanofibers material area weight. A slight addition to nanofibers material another photosensitizer—zinc phthalocyanine (Zn-Pc) results in the intensification of the reaction and increases reaction rate. Increasing the amount of incorporated TPP onto nanofibers material as well as area weight of nanofibers material significantly increases the rate of BuP and BeP photodegradation.

The obtained results allows for the estimation of the kinetic and adsorption parameters. The relation between the

initial degradation rates and initial concentration satisfies Langmuir–Hinshelwood kinetics.

The photosensitized oxidation in a heterogeneous system permits the reuse of the carrier with immobilized photosensitizer, however the multiple usage of them needs still improvements. as the reusability of the photosensitizer by using it in an immobilized form onto insoluble nanofibers carrier is essential from economic and application point of view.

Hydroxylation of parabens is the major reaction that occurs during the photosensitized oxidation. The main photoproducts of the photodegradation of parabens *via* singlet oxygen are 4-hydroxybenzoic acid and monohydroxy parabens.

The toxicity test shows a significant decrease of toxicity after photosensitized oxidation, indicating that reduction of parabens concentration corresponds to an actual detoxification of the treated reaction solution.

References

- [1] P. Meisel, T. Kocher, J. Photochem. Photobiol. B 79 (2005) 159–170.
- [2] L.G. Arnaut, Adv. Inorg. Chem. 63 (2011) 187–233.
- [3] A. Sun, G. Zhang, Y. Xu, Mater. Lett. 59 (2005) 4016–4019.
- [4] Y. Liu, Z. Huang, K. Liu, H. Kelgtermans, W. Dehaen, Z. Wang, X. Zhang, Polym. Chem. 5 (2014) 53–56.
- [5] L. Shao, H. Xie, J. Mo, Z. Yang, Z. Fan, C. Qi, Environ. Eng. Sci. 29 (2012) 807–813.
- [6] N. Liu, G. Sun, Ind. Eng. Chem. Res. 50 (2011) 5326–5333.
- [7] N.A. García, J. Photochem. Photobiol. B 22 (1994) 185–196.
- [8] R. Gerdes, O. Bartels, G. Schneider, D. Wöhrle, G. Schulz-Ekloff, Polym. Advan. Technol. 12 (2001) 152–160.
- [9] D. Drozd, K. Szczubiałka, M. Nowakowska, J. Photochem. Photobiol. A 215 (2010) 223–228.
- [10] M.C. DeRosa, R.J. Crutchley, Coordin. Chem. Rev. 233–234 (2002) 351–371.
- [11] J. Mosinger, O. Jirsak, P. Kubat, K. Lang, B. Mosinger Jr., J. Mater. Chem. 17 (2007) 164–166.
- [12] I. Gonzalez-Marino, J. Benito Quintana, I. Rodriguez, R. Cela, Rapid Commun. Mass Sp. 23 (2009) 1756–1766.
- [13] H. Yamamoto, I. Tamura, Y. Hirata, J. Kato, K. Kagota, S. Katsuki, A. Yamamoto, Y. Kagami, N. Tatarazako, Sci. Total Environ. 410–411 (2011) 102–111.
- [14] M. Terasaki, M. Makino, N. Tatarazako, J. Appl. Toxicol. 29 (2009) 242–247.
- [15] L.L. Dobbins, S. Usenko, R.A. Brain, B.W. Brooks, Environ. Toxicol. Chem. 28 (2009) 2744–2753.
- [16] I. Bazin, A. Gadal, E. Touraud, B. Roig, in: D. Fatta-Kassinos, K., Bester, K. Kummerer (Eds.), Xenobiotics in the Urban Water Cycle: Mass Flows, Environmental Processes, Mitigation and Treatment Strategies (Environmental Pollution), Netherlands, Springer, 2010, p. 245.
- [17] J.M. Brausch, G.M. Rand, Chemosphere 82 (2011) 1518–1532.
- [18] J. Mosinger, K. Lang, P. Kubat, J. Sýkora, M. Hof, L. Pliřtil, B. Mosinger Jr., J. Fluoresc. 19 (2009) 705–713.
- [19] J. Mosinger, K. Lang, L. Pliřtil, S. Jesenská, J. Hostomský, Z. Zelinger, P. Kubát, Langmuir 26 (2010) 10050–10056.
- [20] M. Gmurek, P. Kubat, J. Mosinger, J.S. Miller, J. Photochem. Photobiol. A 223 (2011) 50–56.
- [21] J.M. Larkin, W.R. Donaldson, T.H. Foster, R.S. Knox, Chem. Phys. 244 (1999) 319–330.
- [22] J. Staehelin, J. Hoigne, Environ. Sci. Technol. 19 (1985) 1206–1213.
- [23] I.B. Afanas ev, Superoxide Ion: Chemistry and Biological Implications, vol. 1, CRC Press, Boca Raton, FL, 1989.
- [24] R. Zugle, E. Antunes, S. Khene, T. Nyokong, Polyhedron 33 (2012) 74–81.
- [25] R. Zugle, T. Nyokong, J. Mol. Catal. A-Chem. 366 (2013) 247–253.
- [26] M. Gmurek, J. Mosinger, J.S. Miller, Photochem. Photobiol. S 11 (2012) 1422–1427.
- [27] D.D. Dionysiou, A.P. Khodadoust, A.M. Kern, M.T. Suidan, I. Baudin, J.-M. Laine, Appl. Catal. B: Environ. 24 (2000) 139–155.
- [28] B. Agboola, K.I. Ozoemena, T. Nyokong, J. Mol. Catal. A-Chem. 248 (2006) 84–92.